Available online at www.sciencedirect.com

ScienceDirect

Ceramics International 40 (2014) 2505–2510

CERAMICS INTERNATIONAL

www.elsevier.com/locate/ceramint

Short communication

The correlation between the microstructure and macroscopic properties of (K,Na,Li)(Nb,Ta)O_3 ceramic via rare earth oxide doping

Yongjie Zhao[a,*], Lihua Wang[b], Rongxia Huang[a,*], Rongzheng Liu[a], Heping Zhou[a]

[a]State Key Laboratory of New Ceramics and Fine Processing, School of Materials Science and Engineering, Tsinghua University, Beijing 100084, PR China
[b]Institute of Applied Chemistry, Faculty of Science, Hebei North University, Zhangjiakou 075000, Hebei Province, PR China

Received 25 March 2013; received in revised form 12 July 2013; accepted 15 July 2013
Available online 25 July 2013

Abstract

$Li_{0.05}(Na_{0.51}K_{0.49})_{0.95}(Nb_{0.95}Ta_{0.05})O_3$ (abbreviated as KNNLT) with addition of La_2O_3, CeO_2, respectively, were prepared by a conventional ceramic fabrication technique. X-ray diffraction pattern shows that the coexistence of orthorhombic and tetragonal phase structure for KNNLT was not changed by adding La_2O_3 or CeO_2. SEM observation indicates that these two kind dopants have a remarkable effect on the microstructure of KNNLT ceramics. The $T_{o\text{–}t}$ (temperature for the orthorhombic to tetragonal phase) was shifted toward lower temperature by the addition of rare earth oxide and typical relaxor ferroelectric is demonstrated especially for KNNLT with high content of La_2O_3. An addition of 0.5% CeO_2 could strengthen the piezoelectric and dielectric constant of KNNLT ceramics to some extent. KNNLT ceramics with 0.5% CeO_2 obtain optimum electrical properties: $d_{33}=272$ pC/N, $k_p=45\%$, $\varepsilon_r=784$ and tan $\delta=1.4\%$.

Keywords: A. Ceramics; B. X-ray diffraction; D. Piezoelectricity

1. Introduction

Among the well-known lead-free piezoelectric ceramics systems, $K_xNa_{1-x}NbO_3$ (KNN)-based systems have become a hot area of focus and are recognized as one of the most promising candidates for application. Because they possess good piezoelectric and dielectric properties especially after A-site and/or B-site being partially replaced [1,2]. However, the major drawbacks of KNN ceramics are (i) the need for special treatment of the starting powders due to volatility of alkaline elements, (ii) high sensitivity of the properties to stoichiometry, and (iii) complex densification processes [3]. In order to solve the densification problems, different advanced processes such as spark plasma sintering [4] and hot pressing [5] were developed to promote the sintering, which lead to the enhancement of both the density and the related properties. Although the high piezoelectric constant is induced in KNN-based ceramics by the above mentioned preparation techniques, their complicated preparation process still hinders the practical application.

The doping of metal oxide such as MnO_2, Fe_2O_3, NiO, CuO is a feasible approach to improve the sintering of the piezoceramics [6–12]. The densification of KNN-based materials was evidently improved by the forming of the liquid phase induced by these sintering aids and hence the piezoelectricity of the ceramics could be promoted. These doping mechanisms could be generally divided into two categories and lots of literature have been reported in these two kinds doping mechanisms. One is donor doping and the other is acceptor doping. The doping mechanism is closely related with the ionic radius and electrovalence of doping metal element. The effect of La_2O_3 and CeO_2 on the microstructure and electrical properties of lead-free system such as BNT, BNT–BKT–BT and BT have been investigated [13–15]. However, there are few literature on KNN-based ceramics doped with La_2O_3 or CeO_2 [16]. Due to the similarity of ionic radius between Na^+, K^+ and La^{3+}, Ce^{3+}, it is believed that the introduction of rare earth oxide might bring about considerable influence on the

---

*Corresponding authors. Tel./fax: +86 10 62772549.
E-mail addresses: zhaoyjpeace@gmail.com (Y. Zhao), 9319484@qq.com (R. Huang).

0272-8842/$ - see front matter © 2013 Elsevier Ltd and Techna Group S.r.l. All rights reserved.
http://dx.doi.org/10.1016/j.ceramint.2013.07.072

microstructure and performance. Taking the above into consideration, the research concerning the influence of doping of rare earth oxide on KNN-based materials would be meaningful.

In this work, $Li_{0.05}(Na_{0.51}K_{0.49})_{0.95}(Nb_{0.95}Ta_{0.05})O_3$ (abbreviated as KNNLT) was used as matrix and rare earth oxide (La_2O_3, CeO_2) were selected as dopants. The influences of dopant on the phase structure, the microstructure, the dielectric, ferroelectric and piezoelectric properties of perovskite-type KNN-based ceramics were investigated. The doping mechanism of the rear earth oxide was also discussed. In doing so, we could fully understand that piezoelectric response is dependent on multiple variables such as grain size, and compact degree. These factors have been thoroughly studied and can be used to further modify the magnitude of piezoelectric response once a proper formulation has been identified.

2. Experimental procedure

Lead-free $Li_{0.05}(Na_{0.51}K_{0.49})_{0.95}(Nb_{0.95}Ta_{0.05})O_3$–$x$Ms ($x$= 0, 0.25, 0.5, 0.75, 1 mol% and M: La_2O_3, CeO_2) piezoelectric ceramics were synthesized by a traditional mixed oxide route. The starting powders used in this study were potassium carbonate (K_2CO_3, 99.5%), sodium carbonate (Na_2CO_3, 99.8%), lithium carbonate (Li_2CO_3, 98.5%), tantalum oxide (Ta_2O_5, 99.5%), niobium oxide (Nb_2O_5, 99.5%), lanthanum oxide (La_2O_3, 99.5%) and cerium oxide (CeO_2, 99.5%). After being ball milled in a nylon jar with zirconia balls for 24 h and dried, the stoichiometric $Li_{0.05}(Na_{0.51}K_{0.49})_{0.95}(Nb_{0.95}Ta_{0.05})O_3$ powder was calcinated at 760 °C for 5 h. After the calcination, $Li_{0.05}(Na_{0.51}K_{0.49})_{0.95}(Nb_{0.95}Ta_{0.05})O_3$ and Ms powders were weighted according to the formula and re-milled for 24 h. Then, the powders were dried and pressed into disks using polyvinyl butyral (PVB) as binder. After PVB was burnt off, the pellets were sintered at 1040–1080 °C for 3 h.

The crystal structure of the samples were identified by X-ray powder diffraction (D/MAX-2500, Rigaku, Tokyo, Japan) with a CuKα1 radiation (λ=0.15406 nm). The as sintered surface of the samples were first polished and then scanned at 0.02° intervals of 2θ in the range 20–70°; the scanning speed was 6°/min. The microstructure of the sintered samples was characterized by scanning electron microscopy (SEM, LEO-1530, Oberkochen, Germany). Specimens for the measurement of piezoelectric properties were coated with silver electrodes on both surfaces at 550 °C and then poled in a silicone oil bath under a DC field of 4 kV/mm at room temperature for 20 min. The piezoelectric constant d_{33} was measured using a Piezo-d_{33} meter (PIZEOTEST, PM300, London, UK). Dielectric properties were measured using a LCR meter (TH2816, Tonghui, Changzhou, China) at 1 KHz. The planar electromechanical coupling factor k_p was determined by the resonance–antiresonance method according to IEEE standards using an impedance analyzer (HP 4294A, Hewlett-Packard, Palo Alto, CA). The temperature dependence of the dielectric constant was measured in a temperature-controllable container which was connected to an Agilent 4284 m (Hewlett-Packard, Palo Alto, CA) at 1 kHz.

3. Results and discussion

Fig. 1 shows XRD patterns of KNNLT–xMs sintered at 1080 °C. All the samples exhibit a pure perovskite structure and there is no significant secondary phase found in these diffraction patterns illustrating that Ms have mixed well with KNNLT. Meanwhile, it is observed that there are two distinct peaks (002) and (020) around 45° in the pure KNNLT samples. As the doping amount increases to 0.5%, these two peaks are still evident and just the relative intensities of these two peaks have a little change compared with these of KNNLT sample. At the same time the position of the (002) and (020) peaks, which are associated with the tetragonal degree of the sample, shift toward higher angle and smaller angle, respectively. These two diffraction peaks start to merge when x is 1%. That is to say there is an increase of lattice constant a and decrease of c. In other words, this phenomenon indicates that the volume of the lattice has a slight shrinkage. In KNN-based ceramics, the analysis of the relative intensity of two peaks around $2\theta=45°$ in XRD patterns is an effective way to distinguish the phase structure of ceramics that show orthorhombic and/or tetragonal symmetry at room temperature [17]. When the ceramics are of orthorhombic phase with $a=c>b$, I_{002}/I_{020} equals 2 and the (002) line has a smaller Bragg angle [18], but for KNN-based ceramics of tetragonal phase with $a=b<c$, I_{002}/I_{020} equals 0.5 and the (002) line is also located

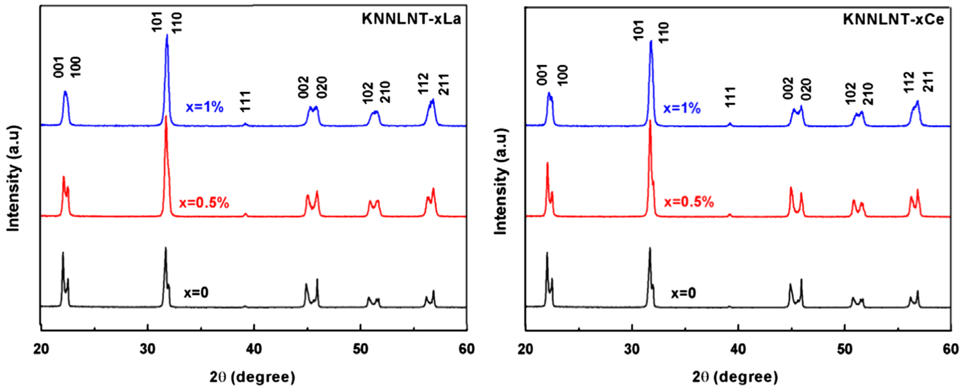

Fig. 1. XRD patterns of KNNLT–xMs ceramics as function of x.

at a smaller Bragg angle. With the above in mind, it easily comes to the conclusion that all the samples possess a coexistence of orthorhombic and tetragonal phase whatever the doping amount is.

The SEM images of the KNNLT–xMs are shown in Fig. 2. For pure KNNLT with $x=0$, the distribution range of grain size is relatively broad. Two kinds of grains are observed: one has a larger diameter (~20 μm), while the other is smaller (~5 μm). For KNNLT doped with La_2O_3, the average grain size of KNNLT sample obviously decreases with the concentration of La_2O_3, and the distribution of grain size gradually becomes uniform. It is reported that the ceramics with a fine grain size and homogeneous microstructure are advantageous for piezoelectric ceramics application, particularly in actuators [19].

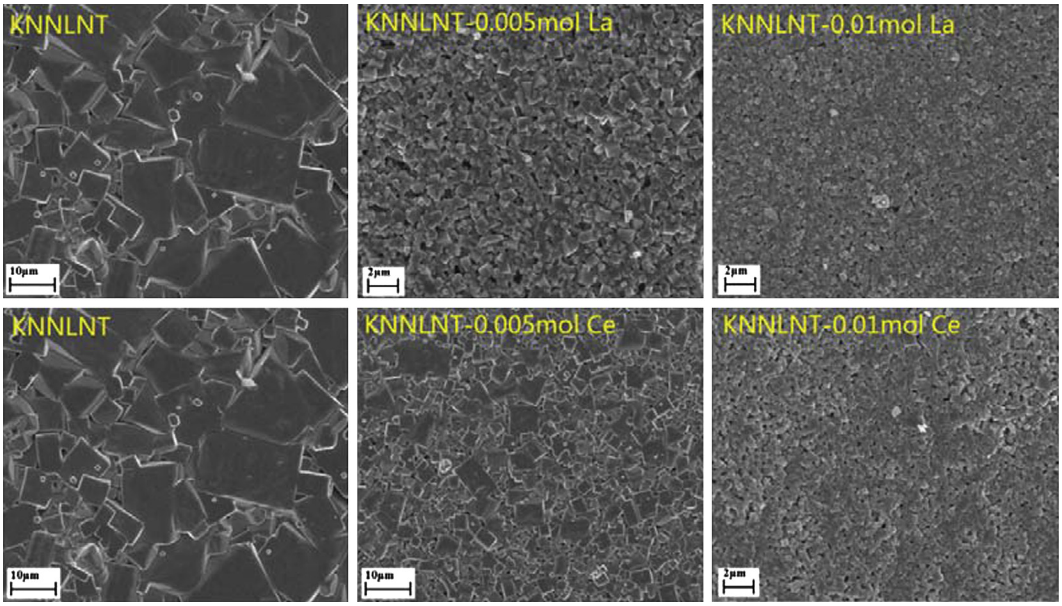

Fig. 2. SEM micrographs of the surface of KNNLT–xMs ceramics sintered at 1080 °C.

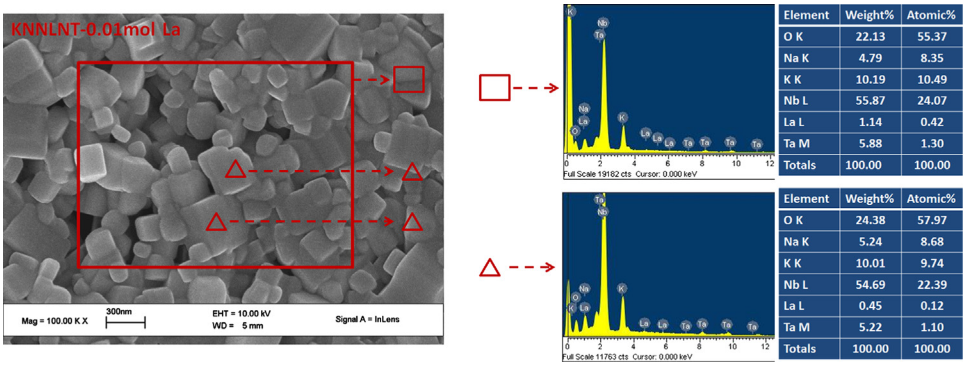

Element	Weight%	Atomic%
O K	22.13	55.37
Na K	4.79	8.35
K K	10.19	10.49
Nb L	55.87	24.07
La L	1.14	0.42
Ta M	5.88	1.30
Totals	100.00	100.00

Element	Weight%	Atomic%
O K	24.38	57.97
Na K	5.24	8.68
K K	10.01	9.74
Nb L	54.69	22.39
La L	0.45	0.12
Ta M	5.22	1.10
Totals	100.00	100.00

Fig. 3. SEM micrograph and EDS results of the KNNLT–1% La sintered at 1080 °C.

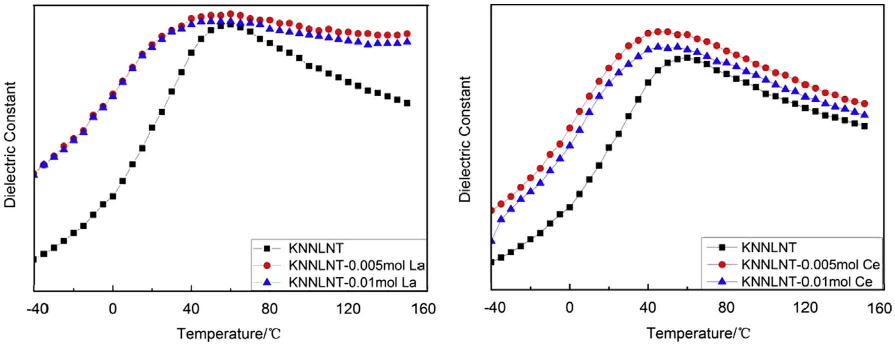

Fig. 4. Temperature dependence of the dielectric constant for KNNLT–xMs ceramics at 1 kHz.

However, distinct pores emerge around the grain boundary as x further increases to 1% and the crystal shape becomes irregular and the grain boundaries become smeared-out. The small grain size of La doping sample is probably due to the segregation of proper quantities of La ions around the grain boundary. The EDS results in Fig. 3 could certify this point. The concentration of La element in the KNNLT grains is lower than that of the average amount in the sample. It is considered that the solubility of La element in the lattice of KNNLT is limited. Consequently, the excessive La element would enrich along the grain boundary resulting in the deterioration of d_{33} for KNNLT with La_2O_3 doping [16].

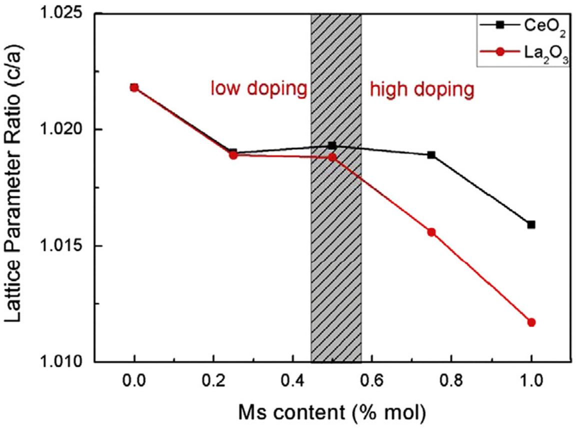

Fig. 5. Relationship of the tetragonality (*c/a*) obtained by XRD versus the content of Ms.

After addition of CeO_2, the average grain size gets reduced and the distribution of grain size becomes more uniform in size (~8 μm). Meanwhile, the specimen′s microstructure becomes more dense when $x=0.5\%$ than that of pure KNNLT without dopant. The reduction in the grain size clearly indicates that CeO_2 is effective in suppressing the melting and abnormal grain growth of KNNLT ceramics during sintering. The sintering kinetics can be described as the lattice diffusion of vacancies from pores to grain boundaries, and the donor doping reduces the diffusion coefficient: the vacancies (e.g. A-site vacancies in our case) created by the doping are supposed to be bound to the impurity ion (e.g. Ce^{3+} in our case). As a result, the mass transportation is weakened and the grain growth is inhibited. It implies that certain amount of CeO_2 is effective in assisting the sintering of the ceramics and hence improving the densification. The highest d_{33} for the KNNLT with 0.5% CeO_2 could prove this consideration. When the content of CeO_2 further increases to 1%, the average grain size is lowered to sub-micrometer and the microstructure becomes obviously porous which is the similar case with 1% La_2O_3 doped KNNLT.

In order to elaborate the influence of the dopant on the room temperature phase structure, the temperature dependence of the dielectric constant from −40 to 150 °C were measured. Fig. 4 shows the temperature dependence of the dielectric behavior for KNNLNT–xMs at 1 kHz. An orthorhombic to tetragonal phase transition, T_{o-t}, is identified near room temperature by the presence of a weak maximum dielectric constant between 25 and 80 °C for all the samples. While the T_{o-t} shifts to a lower temperature and gradually becomes flattened with the

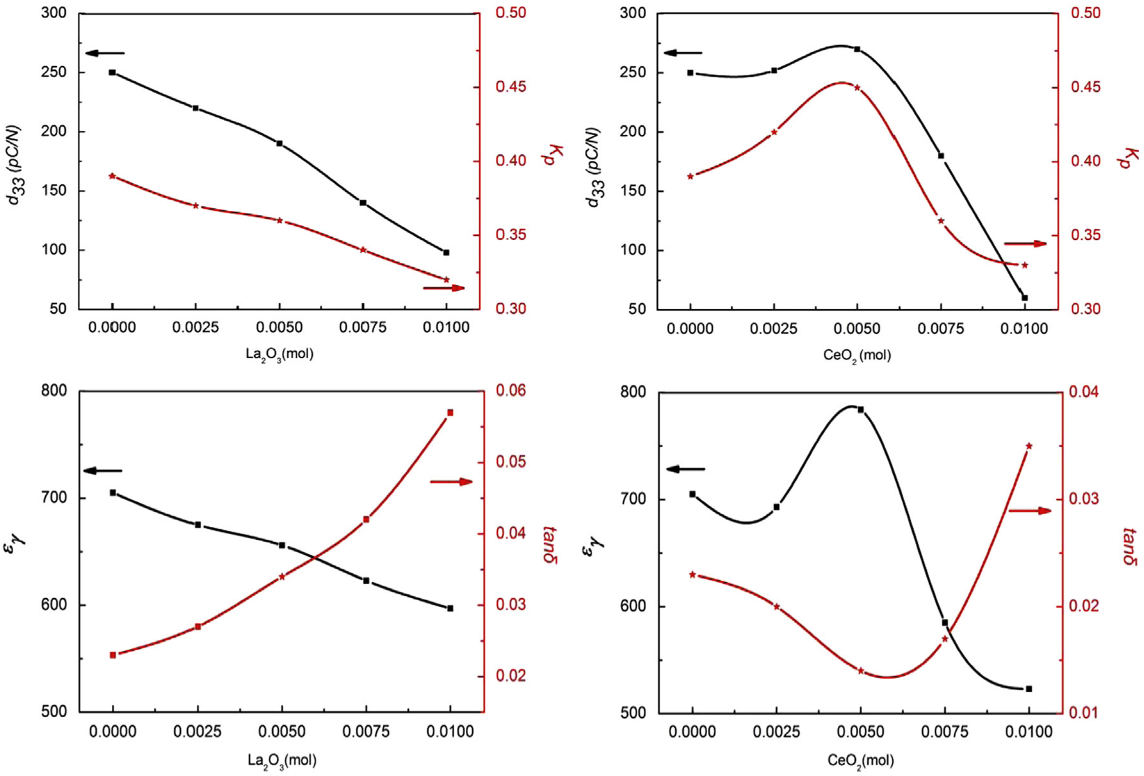

Fig. 6. Variations of the d_{33}, k_p, ε_r and tan δ of KNNLT versus the addition of Ms.

content of Ms especially for La_2O_3 doping. For most ABO_3-type perovskite ferroelectric, it has relaxor feature caused by A and/or B-site substitutions. Fig. 4 also illustrates another phenomenon that the relative dielectric constant increases after the addition of Ms. It supposes that the promotion of relative dielectric constant results from more boundaries induced by the reduction of the average grain size.

Fig. 5 shows the evolution of the lattice parameter ratio (*c/a*) with the doping concentration and different M. The lattice parameters were calculated according to the location of the {200} XRD lines. These two kinds of dopants have a similar case; the value of *c/a* decreases with the content of Ms and the only difference is in the degree of the decrement of *c/a* for two different kinds of dopant. Hence, two cases have been identified relying on the Ms content: (I) for a low doping range (0–0.5%), *c/a* value first evidently decreases and then relatively stabilizes as Ms content increases up to 0.5%; (II) for a high doping range (0.5–1%), the *c/a* value is further reduced, especially for La_2O_3 doping. In the latter circumstances, the doping induces both a shortening of *c* parameter and an increase of *a* and *b* lattice parameters.

Fig. 6 shows the piezoelectric and dielectric properties of KNNLT–*x*Ms specimens. It is found that these parameters are sensitive to the addition of Ms. Generally speaking CeO_2 presents more positive influence on the performance of KNNLT than that of La_2O_3. Each parameter of KNNLT samples with La doping, deteriorates as doping content increases. These deteriorative performances results from the small grain size and loose microstructure as shown in SEM images. However, it is not the same case for KNNLT doped with CeO_2. It is found that with the addition of CeO_2, the piezoelectric constant d_{33} and the electromechanical coupling factor k_p first reach a maximum value at $x = 0.5\%$, and then decrease with further addition of CeO_2. The piezoelectric constant has been altered from 250 pC/N for pure KNNLT to 272 pC/N for 0.5% CeO_2-doping KNNLT. Meanwhile, the electromechanical coupling factor k_p has been increased from 39 to 45%.

It is well known that CeO_2 is a commonly used additive for PZT ceramics [20]. In our work, the addition of CeO_2 also displays the same effect. The mechanism for the effect of CeO_2 in this experiment is very complicated. Ce ion possibly exists both in Ce^{3+} and Ce^{4+} valence states, having a radius of 1.03 Å and 0.92 Å, respectively. Ce^{3+} and Ce^{4+} may replace K^+ (1.33 Å) or Na^+ (1.02 Å) at the A sites and serve as donor-type dopants for the ceramics. On the other hand, Ce^{4+} may also replace Nb^{5+} (0.69 Å) at the B sites of the KNNLT ceramics. Thus, on the basis of ionic radius, the Ce ions could substitute in either A or B-sites. Considering its valence, Ce could either act as a donor-dopant, if introduced in A-site, or as an acceptor-dopant, when introduced in B-site. When Ce occupies A-site, the substitution of A-sites by Ce may cause the slack of KNNLNT lattice and some A-site vacancies. The lattice deformation can make the ferroelectric domains reorientation more easy during electrical poling and leads to the enhancement of piezoelectric properties. Meanwhile, A-sites vacancies could relax the strain caused by the reorientation of domains, the movement of the domains becomes easier and the improvement of piezoelectric properties of the KNNLT ceramics is also favored. The highest value of d_{33} and k_p for KNNLT with 0.5% CeO_2 could be ascribed to the above reasons.

4. Conclusions

KNNLNT–*x*Ms piezoelectric ceramics have been successfully prepared by a conventional mixed-oxide method. Our result reveals that CeO_2 is more effective in promoting the densification and enhancing the ferroelectric, dielectric and piezoelectric properties of the ceramics than La_2O_3. The best performance was achieved in KNNLT with 0.5% CeO_2 doping, giving $d_{33} = 272$ pC/N, $k_p = 45\%$, $\varepsilon_r = 784$ and $\tan\delta = 1.4\%$.

Acknowledgment

This work was supported by the National Natural Science Foundation of China.

References

[1] Y. Saito, H. Takao, T. Tani, K. Nonoyama, T. Hommma, T. Nagaya, M. Nakamura, Lead-free piezoceramics, Nature 432 (2004) 84–87.

[2] R.Z. Zuo, J. Fu, D.Y. Lv, Phase transformation and tunable piezoelectric properties of lead-free $(Na_{0.52}K_{0.48-x}Li_x)(Nb_{1-x-y}Sb_yTa_x)O_3$ system, Journal of the American Ceramic Society 92 (2009) 283–285.

[3] M. Matsubara, T. Yamaguchi, W. Sakamoto, K. Kikuta, T. Yogo, S. Hirano, Processing and piezoelectric properties of lead-free (K,Na) (Nb,Ta) O_3 ceramics, Journal of the American Ceramic Society 88 (2005) 1190–1196.

[4] B. Zhang, J. Li, K. Wang, H. Zhang, Compositional dependence of piezoelectric properties in $Na_xK_{1-x}NbO_3$ lead-free ceramics prepared by spark plasma sintering, Journal of the American Ceramic Society 89 (2006) 1605–1609.

[5] R.E. Jaeger, L. Egerton, Hot pressing of potassium sodium niobates, Journal of the American Ceramic Society 45 (1962) 209–213.

[6] M. Jiang, X. Li, J. Liu, J. Zhu, X. Zhu, L. Li, Q. Chen, J. Zhu, D. Xiao, Structural and electrical properties of Cu-doped $(K_{0.5}Na_{0.5})NbO_3$–$MgTiO_3$ lead-free ceramics, Journal of Alloys and Compounds 479 (2009) L18–L21.

[7] D.M. Lin, K.W. Kwok, H.L.W. Chan, Piezoelectric and ferroelectric properties of $K_xNa_{1-x}NbO_3$ lead-free ceramics with MnO_2 and CuO doping, Journal of Alloys and Compounds 461 (2008) 273–278.

[8] C. Liu, X. Liu, M. Jiang, J. Ma, Microstructure and piezoelectric properties of $Na_{0.5}K_{0.5}NbO_3$–$BiNiO_3$–$LiSbO_3$ lead-free ceramics, Journal of Alloys and Compounds 503 (2010) 209–212.

[9] M.R. Yang, C.S. Hong, C.C. Tsai, S.Y. Chu, Effect of sintering temperature on the piezoelectric and ferroelectric characteristics of CuO doped $0.95(Na_{0.5}K_{0.5})NbO_3$–$0.05LiTaO_3$ ceramics, Journal of Alloys and Compounds 488 (2009) 169–173.

[10] R. Zuo, B. Ma, Y. Liu, Z. Xu, Hardening characteristics and compositional dependence of piezoelectric properties in Cu^{2+} modified $0.52NaNbO_3$–$(0.48-x)KNbO_3-xLiNbO_3$ ceramics, Journal of Alloys and Compounds 488 (2009) 465–468.

[11] Y. Zhao, Y. Zhao, R. Huang, R. Liu, H. Zhou, Enhanced piezoelectric properties of Fe_2O_3–$2TiO_2$ codoped $Li0.05(Na_{0.5}K_{0.5})_{0.95}(Nb_{0.975}Sb_{0.025})O_3$ lead-free ceramics with uniform microstructure, Materials Chemistry Physics 131 (2011) 32–36.

[12] Y. Zhao, Y. Zhao, R. Huang, R. Liu, H. Zhou, Microstructure and piezoelectric properties of CuO-doped $0.95(K_{0.5}Na_{0.5})NbO_3$–0.05Li

$(Nb_{0.5}Sb_{0.5})O_3$ lead-free ceramics, Journal of the European Ceramic Society 31 (2011) 1939–1944.

[13] H. Pan, Y. Hou, X. Chao, L. Wei, Z. Yang, Microstructure and electrical properties of La_2O_3-doped $Bi_{0.5}(Na_{0.68}K_{0.22}Li_{0.1})_{0.5}TiO_3$ lead-free piezoelectric ceramics, Current Applied Physics 11 (2009) 888–892.

[14] M. Chen, W. Chen, H. Liu, H. Kim, B. Ahn, Structure, piezoelectric and ferroelectric properties of La_2O_3 added $(Na_{0.5}Bi_{0.5})_{0.93}Ba_{0.07}TiO_3$ lead-free ceramics, Ferroelectrics 358 (2007) 1005–1010.

[15] S. Choy, X. Wang, H. Chan, C. Choy, $0.75(Bi_{1/2}Na_{1/2})TiO_3$–$0.20(Bi_{1/2}K_{1/2})TiO_3$–$0.05BaTiO_3$ lead-free ceramics with addition of CeO_2, Ferroelectrics 336 (2006) 69–79.

[16] J. Yoo, B. Seo, Dielectric and piezoelectric properties of $(K_{0.5}Na_{0.5})(Nb_{0.96}Sb_{0.04})\ O_3$ ceramics doped with La_2O_3, Ferroelectrics 425 (2011) 106–113.

[17] Y. Guo, K. Kakimoto, H. Ohsato, Phase transitional behavior and piezoelectric properties of $Na_{0.5}K_{0.5}NbO_3 \pm LiNbO_3$ ceramics, Applied Physics Letters 85 (2004) 18.

[18] Y.J. Dai, X.W. Zhang, K.P. Chen, Morphotropic phase boundary and electrical properties of $K1-xNaxNbO_3$ lead-free ceramics, Applied Physics Letters 94 (2009) 042905.

[19] M. Matsubara, K. Kikuta, S. Hirano, Piezoelectric properties of $(K_{0.5}Na_{0.5})(Nb_{1-x}Ta_x)O_3-K_{5.4}CuTa_{10}O_{29}$ ceramics, Journal of Applied Physics 97 (2005) 114105.

[20] B. Jaffe, W.R. Cook, H. Jaffe, Piezoelectric Ceramics, Academic, New York119.